Unusual distance dependences of electron transfer rates

Journal:	*Physical Chemistry Chemical Physics*
Manuscript ID	CP-PER-05-2016-003124.R1
Article Type:	Perspective
Date Submitted by the Author:	13-Jun-2016
Complete List of Authors:	Kuss-Petermann, Martin; University of Basel, Department of Chemistry Wenger, Oliver; University of Basel, Department of Chemistry

Journal Name

PERSPECTIVE

Unusual distance dependences of electron transfer rates

Martin Kuss-Petermann[a] and Oliver S. Wenger[a]

Received 00th January 20xx,
Accepted 00th January 20xx

DOI: 10.1039/x0xx00000x

www.rsc.org/

Usually the rates for electron transfer (k_{ET}) decrease with increasing donor-acceptor distance, but Marcus theory predicts a regime in which k_{ET} is expected to increase when the transfer distance gets longer. Until recently, experimental evidence for such counter-intuitive behavior had been very limited, and consequently this effect is much less well-known than the Gaussian free energy dependence of electron transfer rates leading to the so-called inverted driving-force effect. This article presents the theoretical concepts that lead to the prediction of electron transfer rate maxima at large donor-acceptor distances, and it discusses conditions that are expected to favor experimental observations of such behavior. It continues with a consideration of specific recent examples in which electron transfer rates were observed to increase with increasing donor-acceptor distance, and it closes with a discussion of the importance of this effect in the context of light-to-chemical energy conversion.

Introduction

Due to their low mass, electrons can tunnel over long distances (> 15Å).[1] An exponential decrease of electron transfer rates (k_{ET}) with increasing donor-acceptor distance is usually observed for tunneling, governed by the intervening medium as well as the nature of the donor and the acceptor.[1b, 2] In cases where the intervening medium contains redox-active units, a so-called hopping mechanism can become operative.[3] Hopping is essentially multi-step tunneling and consequently leads to shallower distance dependences, typically with k_{ET} inversely proportional to the donor-acceptor distance.[4] Regardless of which one of the two mechanisms is active, k_{ET} usually decreases with increasing reactant separation. However, Marcus theory predicts a regime in which electron transfer rates should first increase to reach a maximum at a given (optimal) donor-acceptor distance, and then decrease when increasing the reactant separation even further.[5] In principle, this was noted more than 30 years ago,[6] but it remained a largely unknown effect, presumably because experimental evidence for it was elusive. Recent studies have provided direct evidence for electron transfer rate maxima at large donor-acceptor distances,[7] and thus it seemed worthwhile to raise awareness of the underlying theoretical concepts that lead to the prediction of such counter-intuitive behavior. We will identify a set of conditions that should favor the observation of increasing k_{ET} with increasing distance, and we will consider the abovementioned recent studies in this light. Finally, we will discuss the significance of this effect for the conversion of solar light to chemically stored energy.

Basic aspects of electron transfer theory

According to semi-classical theory, electron transfer rates depend on the reaction free energy (ΔG_{ET}^0), the reorganization energy associated with electron transfer (λ), and the electronic coupling (H_{DA}) between the donor and the acceptor (eq. 1).[5]

$$k_{ET} = \sqrt{\frac{\pi}{\hbar^2 \cdot \lambda \cdot k_B \cdot T}} \cdot H_{DA}{}^2 \cdot \exp\left(-\frac{\left(\lambda + \Delta G_{ET}{}^0\right)^2}{4 \cdot \lambda \cdot k_B \cdot T} \right)$$

(eq. 1)

The exponential term in eq. 1 is often referred to as the nuclear factor (κ_N), because it captures the effect of nuclear motions occurring in the course of electron transfer.[8] The remaining factors in eq. 1 can be considered as a product of a frequency factor (ν_n) and an electronic factor (κ_e).

The nuclear factor is responsible for the well-known Gaussian free energy dependence of k_{ET}. In the normal regime of the plot in Figure 1b, k_{ET} increases with increasing driving-force, due to a decreasing activation barrier between the reactant ($f_r(Q)$) and product potential energy wells ($f_p(Q)$). k_{ET} reaches a maximum when $-\Delta G_{ET}^0$ is equal to λ, at which point the reaction proceeds activationless (Figure 1a, middle). A further increase in driving-force entails the re-appearance of an activation barrier, leading to a decrease of k_{ET}. This so-called inverted driving-force effect was predicted by theory,[5] and, after some initial struggle,[9] unambiguous experimental evidence for this phenomenon could be found. Nowadays this effect is well documented and understood.[10]

[a] Department of Chemistry, University of Basel, St. Johanns-Ring 19, 4056 Basel, Switzerland. E-mail: oliver.wenger@unibas.ch

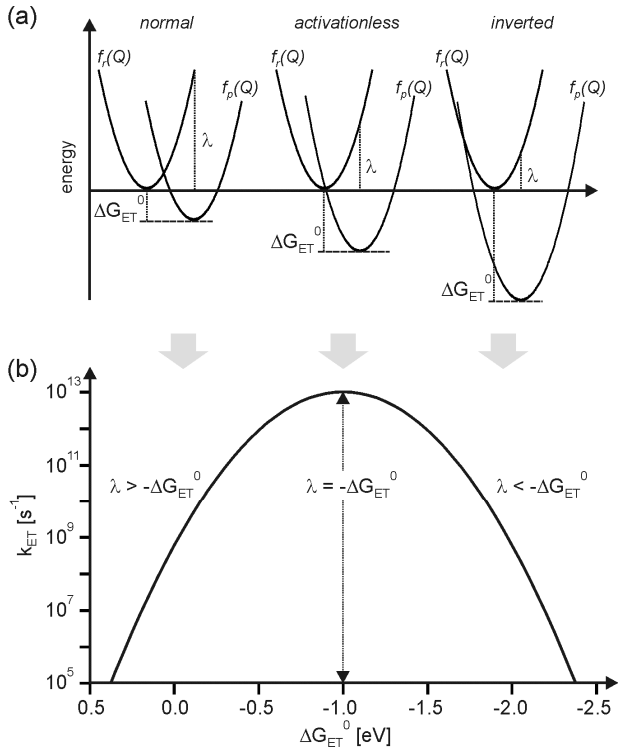

Figure 1. (a) Reactant ($f_r(Q)$) and product potential energy wells ($f_p(Q)$) for electron transfer in three different regimes; (b) dependence of electron transfer rates (k_{ET}) on reaction free energy (ΔG_{ET}^0). A reorganization energy (λ) of 1.0 eV was arbitrarily chosen.

According to superexchange theory, the electronic coupling term H_{DA} can be nonzero even when donor and acceptor are far apart (≥ 15 Å) because the intervening medium (e. g., covalent bridges or solvent molecules) can mediate long-range electronic coupling.[11] H_{DA} usually decreases exponentially with increasing distance (r_{DA}), and the steepness of this decrease is captured by the distance decay parameter (β_{el}).[2b, 3a]

$$H_{DA}(r_{DA}) = H_{DA}^{(0)} \cdot \exp\left(-\beta_{el} \cdot \left(r_{DA} - r_{DA}^{(0)}\right)\right) \quad \text{(eq. 2)}$$

In eq. 2, $H_{DA}^{(0)}$ is the electronic coupling between reactants at van-der-Waals contact distance ($r_{DA}^{(0)}$). Exponential distance dependences of k_{ET} are commonly observed because $k_{ET} \propto H_{DA}^2$ (eq. 1), although strictly speaking this is only to be expected for activationless electron transfer ($-\Delta G_{ET}^0 = \lambda$, see below). Typical distance decay constants for k_{ET} (β) range from 0.4 $Å^{-1}$ for oligo-*p*-phenylene bridges to 1.1 $Å^{-1}$ for proteins and 1.65 $Å^{-1}$ for water,[2b, 4b, 12] but β is governed by the combination of donor, acceptor and intervening medium.[2a, 13] Significantly lower β values were reported for hopping reactions,[14] but in such cases the distance decay constant becomes an entirely phenomenological parameter. Note that the distance decay constant for k_{ET} (β) is twice as large as the distance decay constant for H_{DA} (β_{el}, eq. 2) because $k_{ET} \propto H_{DA}^2$ (eq. 1).

H_{DA} is not the only distance-dependent parameter in eq. 1. While the distance dependence of $-\Delta G_{ET}^0$ is often negligible, that of the reorganization energy (λ) can be substantial.[15] The overall reorganization energy is a sum of inner- (λ_i) and outer-sphere (λ_o) contributions (eq. 3), reflecting the energy required for nuclear reorganization on the donor and the acceptor in the course of electron transfer, as well as reorganization of their chemical environment (e. g., solvent molecules or counter-ions).[5]

$$\lambda = \lambda_i + \lambda_o \quad \text{(eq. 3)}$$

While λ_i is commonly treated as a distance-independent parameter, λ_o strongly depends on r_{DA} and on solvent polarity. In the simplest model, the donor and the acceptor are treated as spheres with radii a_1 and a_2, separated by the distance r_{DA} in a solvent with a given optical (D_{op}) and static dielectric constant (D_s).[5]

$$\lambda_o = \frac{(\Delta e)^2}{4 \cdot \pi \cdot \varepsilon_0} \cdot \left(\frac{1}{2 \cdot a_1} + \frac{1}{2 \cdot a_2} - \frac{1}{r_{DA}}\right) \cdot \left(\frac{1}{D_{op}} - \frac{1}{D_s}\right)$$

(eq. 4)

In eq. 4, Δe is the transferred charge, and D_{op} is related to the refractive index (η) by the relationship $D_{op} = \eta^2$. For a donor and an acceptor with radii of 4 Å in CH_3CN, eq. 4 predicts an increase of λ_o from 0.94 eV to 1.63 eV when increasing r_{DA} from contact distance to 30 Å. More sophisticated models treat the reactants as ellipsoids and permit more precise predictions,[16] but the key point is that λ_o increases with increasing r_{DA} and thus opposes the distance dependence of H_{DA}.

Consequences of opposing distance dependences of H_{DA} and λ_o

Driving-force dependence parabola such as that in Figure 1b can be calculated as a function of r_{DA} using equations 1 – 4.[17] For spherical donors and acceptors with radii (a_1, a_2) of 4 Å in CH_3CN (η = 1.3341, D_s = 35.7) at 298 K, we assumed $H_{DA}^{(0)}$ = 200 cm^{-1}, β = 0.8 $Å^{-1}$, and λ_i = 0.1 eV. The Marcus parabola obtained for r_{DA} = 8, 11, and 21 Å are shown in Figure 2. The decrease of H_{DA} with increasing r_{DA} (eq. 2) causes a downward shift, while the increase of λ (eqs. 3, 4) displaces the parabola to the right, because the activationless point is reached when $-\Delta G_{ET}^0 = \lambda$ (eq. 1). The two horizontal lines in Figure 2 illustrate that at constant driving-force very different distance dependences for k_{ET} can result, depending on the exact driving-force. At ΔG_{ET}^0 = -1.0 eV, k_{ET} decreases with increasing r_{DA}, whereas at ΔG_{ET}^0 = -2.0 eV there is an increase of k_{ET} between 8 and 11 Å followed by a decrease at 21 Å. In other words, there are regimes in which one expects electron transfer rate maxima at large donor-acceptor distances.

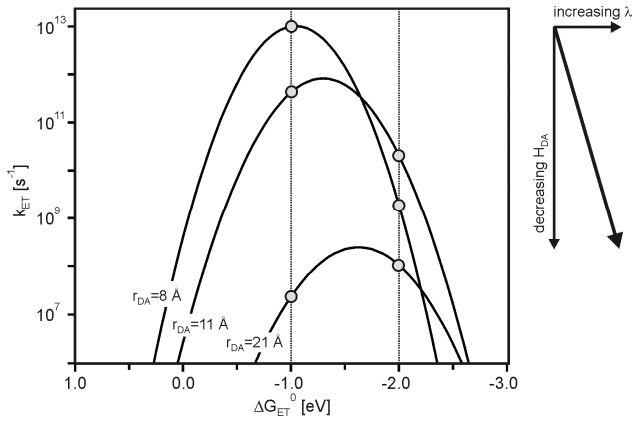

Figure 2. Driving-force dependence of electron transfer rates (k_{ET}) at three different donor-acceptor distances (r_{DA}). Calculated using equations 1 – 4 and the following parameters: $H_{DA}^{(0)}$ = 200 cm^{-1}, β = 0.8 $Å^{-1}$, λ_i = 0.1 eV, $a_1 = a_2$ = 4 Å, η = 1.3341 ($D_{op} = \eta^2$), D_s = 35.7 (values for CH_3CN).

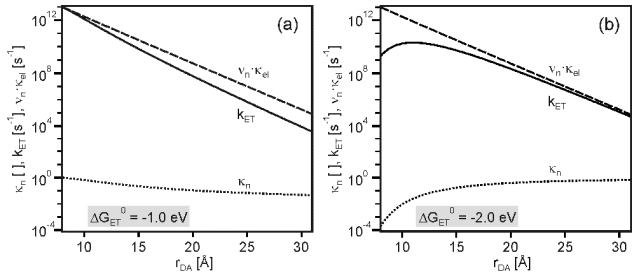

Figure 3. Distance dependences of electron transfer rates (k_{ET}, solid lines), the nuclear factor (κ_n, dotted lines), and the product of frequency factor and electronic factor ($\nu_n \cdot \kappa_{el}$, dashed lines). Calculated using equations 1 – 4 and the same set of parameters as for Figure 2, once with ΔG_{ET}^0 = -1.0 eV (a) and once with ΔG_{ET}^0 = -2.0 eV (b).

As seen from Figure 3a, at ΔG_{ET}^0 = -1.0 eV there is only a minor deviation from strictly exponential dependence of k_{ET} on r_{DA}, because the distance dependence of the nuclear factor (κ_N) is weak in this case (dotted line), and the contribution from $\nu_n \cdot \kappa_e$ is dominant (dashed line). At ΔG_{ET}^0 = -2.0 eV (Figure 3b), however, the distance dependences of κ_n and $\nu_n \cdot \kappa_e$ oppose each other, leading to maximal k_{ET} at 11 Å. The reason for this is that the $(\lambda + \Delta G_{ET}^0)^2$ term in eq. 1 decreases with increasing λ when $-\Delta G_{ET}^0 > \lambda$ (the sum of ΔG_{ET}^0 and λ becomes less negative), and this makes the distance dependences of reactions occurring in the inverted driving-force regime fundamentally different from those taking place in the normal regime. From Figure 2 it is evident that the increase of k_{ET} with increasing r_{DA} at relatively short distances relies on a decrease of the ratio $-\Delta G_{ET}^0 / \lambda$ from values clearly above 1.0 to values closer to 1.0. In other words, at ΔG_{ET}^0 = -2.0 eV the reaction for r_{DA} = 11 Å is less deeply inverted than for r_{DA} = 8 Å.

While the parameters used above (Figures 2, 3) are not unusual in any regard, their choice is somewhat arbitrary. In the following we discuss trends that emerge from variation of these parameters with particular emphasis on identifying conditions that favor the appearance of electron transfer rate maxima at large r_{DA}.

The weaker the contribution of $\nu_n \cdot \kappa_e$ is, the stronger the rate enhancing effect of κ_n can become hence low β values are favorable. This is illustrated in Figure 4a which shows the distance dependence of k_{ET} at ΔG_{ET}^0 = -2.0 eV for β = 0.4, 0.8, and 1.2 $Å^{-1}$ with all other parameters kept identical as in Figure 3.

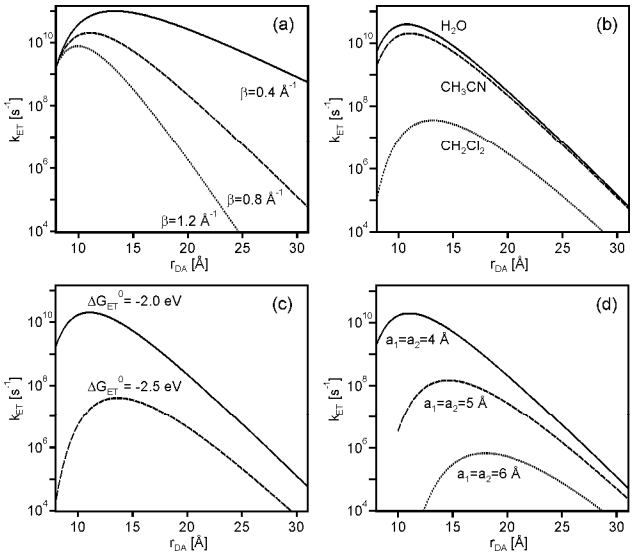

Figure 4. Distance dependence of k_{ET} as a function of different parameters: (a) as a function of distance decay constant (β); (b) as a function of solvent; (c) as a function of driving-force (ΔG_{ET}^0); (d) as a function of donor / acceptor radii (a_1, a_2). Unless otherwise noted the calculations were performed for CH_3CN (η = 1.3341, D_s = 35.7). $H_{DA}^{(0)}$ = 200 cm^{-1} and λ_i = 0.1 eV was used in all cases, the other parameters were as follows: (a) ΔG_{ET}^0 = -2.0 eV, $a_1 = a_2$ = 4 Å; (b) ΔG_{ET}^0 = -2.0 eV, $a_1 = a_2$ = 4 Å, β = 0.8 $Å^{-1}$; (c) $a_1 = a_2$ = 4 Å, β = 0.8 $Å^{-1}$; (d) ΔG_{ET}^0 = -2.0 eV, β = 0.8 $Å^{-1}$. For the calculations in (b), η = 1.3330 and D_s = 80.1 were used for H_2O, and η = 1.4241 and D_s = 8.93 were used for CH_2Cl_2.

An increase in solvent dielectric constant entails larger outer-sphere reorganization energies (eq. 4), lowering the ratio between $-\Delta G_{ET}^0$ and λ. As noted above, the increase of k_{ET} with increasing r_{DA} at relatively short distances relies on a changeover from deeply inverted to less inverted electron transfer, and if the ratio $-\Delta G_{ET}^0 / \lambda$ is close to 1.0 already at contact distance, then expectable effect is less important. Thus, when going from CH_2Cl_2 to CH_3CN and H_2O, the increase of k_{ET} between contact and optimal distance calculated for ΔG_{ET}^0 = -2.0 eV with the parameter set from above amounts to factors of 311, 11, and 7, respectively (Figure 4b). In practice however, a change in solvent will usually lead to changes in both ΔG_{ET}^0 and λ.[9]

In a given solvent, an increase in driving-force at constant λ amplifies the observable effect because the reaction gets more deeply inverted. For example, the rate increase between contact and optimal distance in CH_3CN increases from a factor of 11 to a factor of 1636 when going from ΔG_{ET}^0 = -2.0 eV to ΔG_{ET}^0 = -2.5 eV (Figure 4c), and in CH_2Cl_2 the same driving-force change entails an increase in acceleration factor from 311 to $8.08 \cdot 10^5$ when keeping all other parameters constant.

An increase of the donor and acceptor radii (a_1, a_2) leads to smaller λ_o in a given solvent, making the ratio $-\Delta G_{ET}^0 / \lambda$ larger

when keeping all other parameters constant. In consequence, for ΔG_{ET}^{0} = -2.0 eV the rate acceleration between contact and optimal distance in CH_3CN increases by factors of 11, 45, and 146 when increasing a_1 and a_2 from 4 to 5 to 6 Å (Figure 4d).

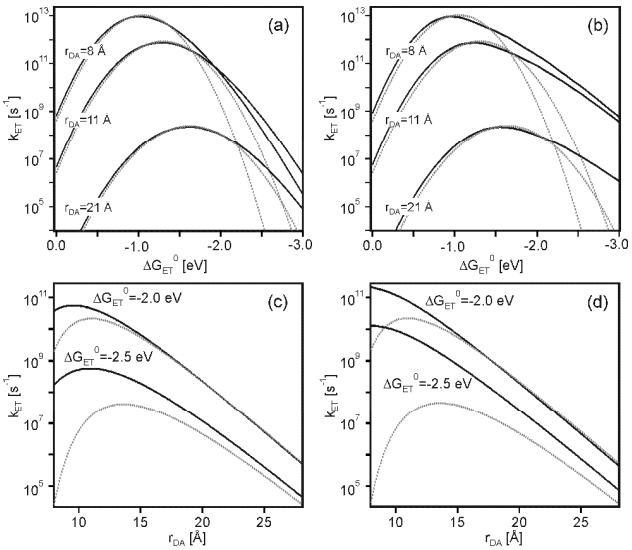

Figure 5. Effect of nuclear tunneling on driving-force dependences at constant distances (a, b) and on distance dependences at constant driving-forces (c, d) in CH_3CN. The dotted lines in (a, b) are the same as in Figure 2, reflecting the situation in absence of nuclear tunneling. The solid lines were calculated using equations 2 – 5 (i. e., including nuclear tunneling effects) and the following input parameters: $H_{DA}^{(0)}$ = 200 cm^{-1}, β = 0.8 Å^{-1}, λ_i = 0.1 eV, $a_1 = a_2$ = 4 Å, and (a) $\hbar\omega$ = 200 meV (1613 cm^{-1}) or (b) $\hbar\omega$ = 450 meV (3630 cm^{-1}). Note that S = λ_i / $\hbar\omega$. The dotted lines in (c, d) are the same as in Figure 4c, reflecting the situation in absence of nuclear tunneling. The solid lines in (c, d) reflect the situation in presence of nuclear tunneling using the same input parameters as for (a, b), once with $\hbar\omega$ = 200 meV (c) and once with $\hbar\omega$ = 450 meV (d).

Influence of nuclear tunneling

Since the rate maxima at large r_{DA} rely on reactions which occur in the inverted driving-force regime, nuclear tunneling is expected to influence the magnitude of this effect. Nuclear tunneling relies on the overlap of vibrational wavefunctions between the reactant and product state. In the so-called Jortner model (eq. 5), this vibrational overlap is captured by the Franck-Condon (FC) factor.[18]

$$k_{ET} = \sqrt{\frac{\pi}{\hbar^2 \cdot \lambda_o \cdot k_B \cdot T}} \cdot {H_{DA}}^2 \cdot (FC) \quad \text{(eq. 5a)}$$

$$(FC) = \sum_{\nu'} \exp(-S) \cdot \frac{S^{\nu'}}{\nu'!} \cdot \exp\left(- \frac{\left(\lambda_o + \nu' \cdot \hbar\omega + \Delta G_{ET}{}^{0}\right)^2}{4 \cdot \lambda_o \cdot k_B \cdot T} \right)$$

(eq. 5b)

In eq. 5, S is the Huang-Rhys parameter describing the displacement of reactant and product potential wells along the reaction coordinate, $\hbar\omega$ is the energy of the vibrational mode responsible for the inner-sphere reorganization occurring with electron transfer, and ν' is the quantum number of the vibrational acceptor level on the product potential energy well. The Huang-Rhys parameter is given by S = λ_i / $\hbar\omega$, where λ_i is the inner-sphere reorganization energy given as a sum of all the coupled intramolecular vibrations which lead to nuclear rearrangements.

The effect of the Jortner model on the Marcus parabola from Figure 2 is to make them unsymmetrical, because nuclear tunneling speeds up electron transfer in the inverted region. This is illustrated in Figure 5a/b (solid lines) where the same parameters as in Figure 2 were used (λ_i = 0.1 eV), but now employing eq. 5 with (a) $\hbar\omega$ = 200 meV (1613 cm^{-1}) and (b) $\hbar\omega$ = 450 meV (3630 cm^{-1}). It is evident from these plots that at constant driving-force, nuclear tunneling weakens the effect of rate maxima at large donor-acceptor separations. This is even more obvious from Figure 5c/d which compares the distance dependences of k_{ET} in absence (dotted lines) and in presence (solid lines) of nuclear tunneling at different driving-forces. For $\hbar\omega$ = 450 meV (Figure 5d), the effect of rate maxima at large donor-acceptor separations has disappeared even at ΔG_{ET}^{0} as high as -2.5 eV.

Experimental observations of increasing electron transfer rates with increasing donor-acceptor distance

The vast majority of experimental studies reported on electron transfer rates which simply decrease with increasing donor-acceptor separation, either due to superexchange tunneling or multi-step hopping.[2a-c, 3a, 12a, 13a, 13b, 19] Some early studies on electron transfer between randomly dispersed donors and acceptor in glassy matrices had invoked the theoretical framework discussed above as a possible explanation for the difficulties associated with observing the inverted driving-force regime in bimolecular electron transfer.[20] However, to the best of our knowledge, until very recently direct experimental evidence for the effect pointed out in 1984 by Brunschwig, Ehrenson and Sutin had been elusive.[6]

We recently reported on 3 series of donor-photosensitizer-acceptor triads in which the rates for thermal electron-hole recombination after initial photoexcitation exhibited maxima at large donor-acceptor distances.[7] Specifically, the ruthenium(II) photosensitizers of the triads in Figure 6a were excited selectively at 532 nm, and this lead rapidly to a triarylamine radical cation (TAA^+) and an anthraquinone radical anion (AQ^-).[21] Intramolecular thermal charge recombination was then monitored as a function of distance through variation of the *p*-xylene spacer lengths (n = 1-3). The important finding was that the rate constant for charge-recombination increased by a factor of 6-10 between the triads with n = 1 and those with n = 2, i. e., an increase in donor-acceptor distance by 8.6 Å was accompanied by an increase of k_{ET} by almost one order of magnitude (right part of Figure 6). Upon further distance elongation, k_{ET} then decreased by 2 orders of magnitude (Table 1). In other words, there were rate maxima at a donor-acceptor distance of 30.6 Å.

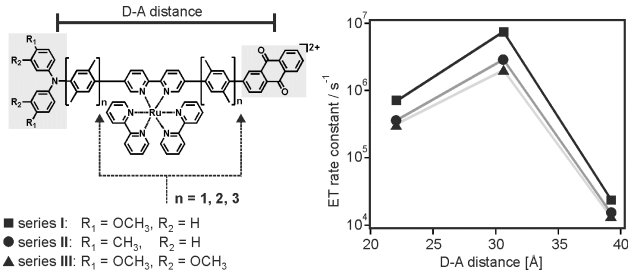

Figure 6. Chemical structure of donor-photosensitizer-acceptor triads and observation of electron transfer rate maxima as a function of donor-acceptor distance.[7] Reprinted with permission from M. Kuss-Petermann, O. S. Wenger, J. Am. Chem. Soc. 2016, 138, 1349. Copyright 2016 American Chemical Society.

Table 1. Rate constants for electron transfer (k_{ET}) from AQ^- to TAA^+ in the three triad series from Figure 6 in 1:1 (v:v) CH_3CN/H_2O at 20 °C.[7] *n* is the number of *p*-xylene bridging units, r_{DA} is the donor-acceptor distance.

n	r_{DA} [Å]	series I	series II	series III
1	22.0	$(3.58\pm0.36)\cdot10^5$	$(6.90\pm0.69)\cdot10^5$	$(3.13\pm0.31)\cdot10^5$
2	30.6	$(2.87\pm0.29)\cdot10^6$	$(7.41\pm0.74)\cdot10^6$	$(2.00\pm0.20)\cdot10^6$
3	39.2	$(1.53\pm0.15)\cdot10^4$	$(2.43\pm0.24)\cdot10^4$	$(1.34\pm0.13)\cdot10^4$

This unusual observation was explained in the framework of the model illustrated by Figure 2.[6] Temperature-dependent studies indicated that charge-recombination in the triads with n = 2 proceeded in activationless manner, whereas in the systems with n = 1 or n = 3 this process required significant thermal activation. Keeping in mind that the reorganization energy commonly increases with increasing donor-acceptor distance (eq. 4), the temperature-dependent studies were interpreted in terms of a changeover from the inverted regime (n = 1) to activationless (n = 2) and normal electron transfer (n = 3). This changeover is illustrated by the potential well diagrams in Figure 7. The reaction free energy (ΔG_{ET}^0) is essentially distance-independent in these systems, but the increase in reorganization energy (λ) then leads to decreasing ratios of $-\Delta G_{ET}^0 / \lambda$ with increasing distance, manifesting in the abovementioned changeover between different regimes. In the investigated triads $-\Delta G_{ET}^0 / \lambda$ varied from ~1.4 (n = 1) to ~0.5 (n = 3).

Two aspects of these studies deserve further comment. First of all, the increase of λ was very large, particularly between the triads with n = 2 (λ = 1.3-1.5 eV) and n = 3 (λ = 2.0-2.2 eV). In principle, reorganization energies up to ~2.0 eV in CH_3CN/H_2O mixtures can be explained adequately by the breakage of hydrogen-bonds between anthraquinone radical anion and solvent molecules,[22] but it is not obvious why the increase between n = 2 and n = 3 is so large. Second, the decrease of the electronic coupling matrix element (H_{DA}) with increasing distance was extremely shallow, in fact nearly distance-independent for some of the triad systems considered until now. This finding is all the more astonishing in light of prior studies of the distance dependence of electron transfer through oligo-*p*-xylenes which provided β-values in the range 0.52-0.76 $Å^{-1}$.[23] It is likely that the 2,2'-bipyridine ligand unit and its coordinated ruthenium(II) complex have a strong influence on the electronic donor-acceptor coupling, and there was direct evidence for significant π-conjugation between this 2,2'-bipyridine ligand and its adjacent *p*-xylene groups.[7] Nevertheless, the extent to which H_{DA} is insensitive to distance remains astonishing.

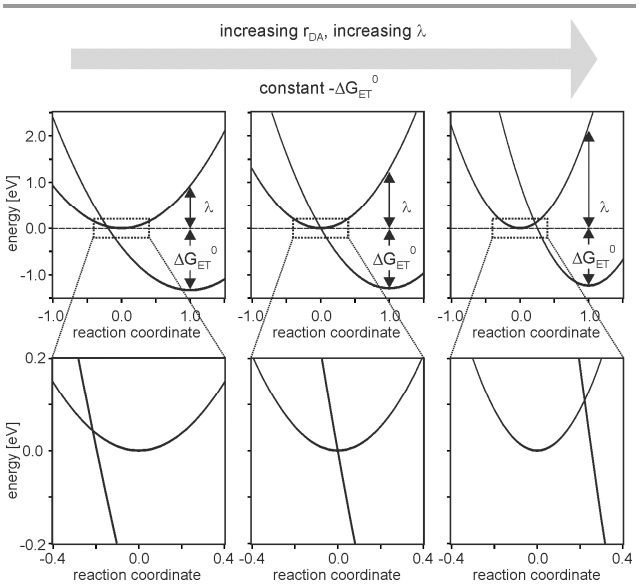

Figure 7. Harmonic potential energy wells for reactant and product states of charge-recombination between AQ^- and TAA^+ in the triads from Figure 6. The lower half shows zooms of the key regions from the upper half. Reprinted with permission from M. Kuss-Petermann, O. S. Wenger, J. Am. Chem. Soc. 2016, 138, 1349. Copyright 2016 American Chemical Society.

The harmonic potential well model (Figure 2) used to account for the observation of rate maxima at large donor-acceptor distances is almost certainly too simplistic to grasp the full complexity of the problem, and once more experimental data will be available, then it will be worthwhile considering more sophisticated theoretical treatments. The finding of unusually large reorganization energies and very shallow distance dependences of H_{DA} might have a common origin, for example it is possible that λ and H_{DA} cannot be considered mutually fully independent parameters in some of these systems.

Consequences for light-to-chemical energy conversion

For solar energy conversion one is interested in fast (efficient) photoinduced charge-separation combined with slow (inefficient) thermal charge-recombination. Photoinduced charge-separation reactions commonly occur in the normal regime in which $-\Delta G_{ET}^0 < \lambda$. Under these conditions, k_{ET} simply decreases with increasing r_{DA} hence photoinduced charge-separation is fastest between reactants that are in van-der-Waals contact (upper half of Figure 8). In terms of converting light into chemical energy it is then desirable for the products (oxidized donor, D^+, and reduced acceptor, A^-) to diffuse away from one another without undergoing direct charge-recombination. However, charge-recombination frequently

occurs in the inverted regime in which $-\Delta G_{ET}^0 > \lambda$, and consequently the rate for this undesired reaction can actually increase with increasing separation between D^+ and A^- to reach an optimum at a critical distance (lower half of Figure 8). In other words, as D^+ and A^- diffuse away from each other, the probability for them to undergo undesired charge-recombination actually increases up to a critical distance, and only beyond this point there is a decrease. This effect can severely limit the overall efficiency of light-to-chemical energy conversion.

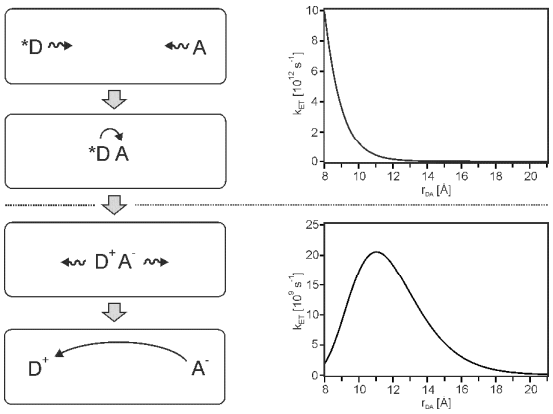

Figure 8. Left: Diffusive motion leading to the formation of an encounter complex between an excited donor (*D) and an acceptor (A), followed by photoinduced charge-separation. Diffusion then separates the photoproducts spatially, but since charge-recombination is usually highly exergonic it can exhibit a rate maximum at large distances. Right: Distance dependences for weakly exergonic (ΔG_{ET}^0 = - 1.0 eV, top) and strongly exergonic reactions (ΔG_{ET}^0= -2.0 eV, bottom), calculated using equations 1 – 4 and the same parameters as in Figure 2.

Nuclear factor contributions to the distance dependence of k_{ET} in other systems

Many studies on proteins focused on activationless electron transfer because under this condition it is possible to isolate the contribution of the electronic factor to the distance dependence of k_{ET}.[12b] In cases in which the electron transfer is not activationless, electronic and nuclear factors both contribute to the distance dependence of k_{ET}, and there are a few examples in the literature where the contribution of the nuclear factor became particularly evident. Electron transfer across proline bridges in the three series of dyads from Figure 9 was triggered by pulse radiolysis through reduction of the Os(III) species (Os-Co, Os-Ru series) or the $Ru(bpy)_3^{2+}$ unit (Ru-Co series).[24] The distance dependence of k_{ET} deviates significantly from strictly mono-exponential behavior in all three dyad series, and this was interpreted in terms of strongly distance-dependence nuclear (κ_n) and electronic factors (κ_e).[24] Using an approach that expresses the activation parameters for intramolecular electron transfer in terms of transition state theory, activation enthalpies ($\Delta H^{\ddagger}$) and activation entropies ($\Delta S^{\ddagger}$) were determined. It was then argued that under certain assumptions,[15a] the slope of $\Delta S^{\ddagger}/R$ versus distance (R is the universal gas constant) yields the distance decay constant (β) of the electronic factor, whereas the slope of $-\Delta H^{\ddagger}/R{\cdot}T$ versus distance provides the distance decay constant (γ) for the nuclear factor.[24] For the Os-Ru dyads from Figure 9 the assumptions of this approach were justified,[24] and the distance dependence of κ_n turned out to be stronger than that of κ_e (γ = 0.91 $Å^{-1}$ vs. β = 0.68 $Å^{-1}$).[15a] This is a remarkable finding and an instructive example of how important nuclear factor contributions to the distance dependence of k_{ET} can be. The parallel to our triads is that we also observe strongly distance dependent nuclear factors (Figure 7).

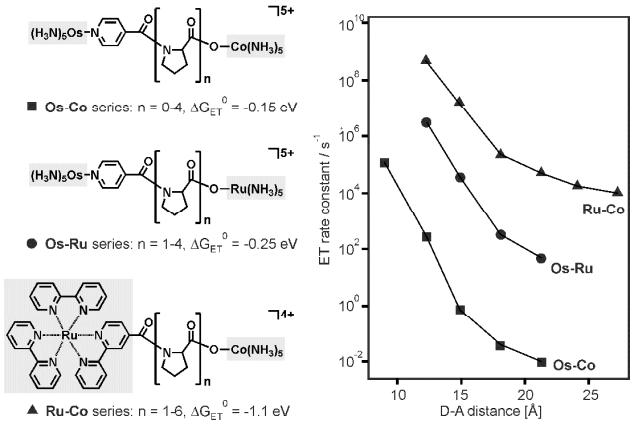

Figure 9. Donor-acceptor dyads with proline bridges and distance dependences of k_{ET} after reduction of the donor moieties (left-hand sides) with pulse radiolysis. The change from Os-Co [25] to Os-Ru [26] and Ru-Co systems [27] allowed a change in driving-force (ΔG_{ET}^0) from -0.15 to -1.1 eV.

In the Os-Ru dyads from Figure 9 the reorganization energy increased from 1.22 eV (n = 1) to 1.52 eV (n = 2) to finally 1.78 eV (n = 3), whereas in the case of our own triads from Figure 6 the change in λ was even larger (0.9 – 2.2 eV, see above) but this occurred over a significantly greater distance range (17.2 Å compared to 5.9 Å). The driving-force associated with intramolecular electron transfer in the Os-Ru dyads is relatively small (ΔG_{ET}^0 = -0.25 eV).[26] Consequently, a changeover in the ratio between $-\Delta G_{ET}^0$ and λ from values below 1.0 (indicative of inverted behavior) to values above 1.0 (signaling electron transfer in the normal regime) was not observable in these systems.

Nevertheless, the dyads from Figure 9 represent early examples of clear-cut cases in which contributions of the nuclear factor to the distance dependence of k_{ET} became observable. In other early studies, the model illustrated by Figure 2 was invoked to explain the difference in the distance dependences of weakly exergonic charge-separation reactions and strong exergonic charge-recombination processes.[15c]

Conclusions

There are two counter-intuitive scenarios for electron transfer: (i) decreasing rates with increasing driving-force (at constant donor-acceptor distance), and (ii) increasing rates with increasing donor-acceptor distances (at constant driving-force). The first scenario, usually called the inverted driving-force effect,[5] is very well known and experimentally well

documented.[10] The second scenario, while predicted by theory a long time ago,[6] is comparatively little known, presumably because unambiguous experimental evidence for it was found only very recently.[7]

Increasing rates with increasing donor-acceptor distances can result from increasing (outer-sphere) reorganization energies (λ_o) in the inverted driving-force regime, leading to lower activation barriers at constant driving-force. Our recent experimental studies demonstrated that it is even possible to induce a changeover from the inverted to the normal regime by increasing the donor-acceptor separation.[7] When dealing with photoinduced electron transfer reactions, this effect becomes important for light-to-chemical energy conversion.

Acknowledgements

Financial support by the Swiss National Science Foundation through grant number 200021-146231/1 is gratefully acknowledged.

Notes and references

1 (a) D. De Vault and B. Chance, *Biophys. J.*, 1966, **6**, 825-847; (b) J. R. Winkler and H. B. Gray, *J. Am. Chem. Soc.*, 2014, **136**, 2930-2939.

2 (a) B. Albinsson, M. P. Eng, K. Pettersson and M. U. Winters, *Phys. Chem. Chem. Phys.*, 2007, **9**, 5847-5864; (b) H. B. Gray and J. R. Winkler, *Proc. Natl. Acad. Sci. U. S. A.*, 2005, **102**, 3534-3539; (c) M. Natali, S. Campagna and F. Scandola, *Chem. Soc. Rev.*, 2014, **43**, 4005-4018; (d) F. D. Lewis, J. Q. Liu, W. Weigel, W. Rettig, I. V. Kurnikov and D. N. Beratan, *Proc. Natl. Acad. Sci. U. S. A.*, 2002, **99**, 12536-12541; (e) O. S. Wenger, *Inorg. Chim. Acta*, 2011, **374**, 3-9; (f) D. C. O'Hanlon, B. W. Cohen, D. B. Moravec, R. F. Dallinger and M. D. Hopkins, *J. Am. Chem. Soc.*, 2014, **136**, 3127-3136; (g) A. Helms, D. Heiler and G. McLendon, *J. Am. Chem. Soc.*, 1992, **114**, 6227-6238; (h) L. T. Calcaterra, G. L. Closs and J. R. Miller, *J. Am. Chem. Soc.*, 1983, **105**, 670-671; (i) H. Oevering, M. N. Paddon-Row, M. Heppener, A. M. Oliver, E. Cotsaris, J. W. Verhoeven and N. S. Hush, *J. Am. Chem. Soc.*, 1987, **109**, 3258-3269; (j) S. V. Rosokha, D.-L. Sun and J. K. Kochi, *J. Phys. Chem. A*, 2002, **106**, 2283-2292.

3 (a) M. Cordes and B. Giese, *Chem. Soc. Rev.*, 2009, **38**, 892-901; (b) C. Shih, A. K. Museth, M. Abrahamsson, A. M. Blanco-Rodriguez, A. J. Di Bilio, J. Sudhamsu, B. R. Crane, K. L. Ronayne, M. Towrie, A. Vlček, J. H. Richards, J. R. Winkler and H. B. Gray, *Science*, 2008, **320**, 1760-1762; (c) C. Lambert, G. Nöll and J. Schelter, *Nat. Mater.*, 2002, **1**, 69-73; (d) M. Cordes, A. Kottgen, C. Jasper, O. Jacques, H. Boudebous and B. Giese, *Angew. Chem. Int. Ed.*, 2008, **47**, 3461-3463; (e) J. C. Genereux and J. K. Barton, *Chem. Rev.*, 2010, **110**, 1642-1662; (f) V. Lloveras, J. Vidal-Gancedo, T. M. Figueira-Duarte, J. F. Nierengarten, J. J. Novoa, F. Mota, N. Ventosa, C. Rovira and J. Veciana, *J. Am. Chem. Soc.*, 2011, **133**, 5818-5833; (g) K. E. Linton, M. A. Fox, L. O. Palsson and M. R. Bryce, *Chem.-Eur. J.*, 2015, **21**, 3997-4007.

4 (a) W. B. Davis, W. A. Svec, M. A. Ratner and M. R. Wasielewski, *Nature*, 1998, **396**, 60-63; (b) O. S. Wenger, *Chem. Soc. Rev.*, 2011, **40**, 3538-3550.

5 R. A. Marcus and N. Sutin, *Biochim. Biophys. Acta*, 1985, **811**, 265-322.

6 B. S. Brunschwig, S. Ehrenson and N. Sutin, *J. Am. Chem. Soc.*, 1984, **106**, 6858-6859.

7 (a) M. Kuss-Petermann and O. S. Wenger, *Angew. Chem. Int. Ed.*, 2016, **55**, 815-819; (b) M. Kuss-Petermann and O. S. Wenger, *J. Am. Chem. Soc.*, 2016, **138**, 1349-1358.

8 N. Sutin, *Acc. Chem. Res.*, 1982, **15**, 275-282.

9 D. Rehm and A. Weller, *Isr. J. Chem.*, 1970, **8**, 259-271.

10 (a) G. L. Closs and J. R. Miller, *Science*, 1988, **240**, 440-447; (b) M. R. Wasielewski, M. P. Niemczyk, W. A. Svec and E. B. Pewitt, *J. Am. Chem. Soc.*, 1985, **107**, 1080-1082; (c) L. S. Fox, M. Kozik, J. R. Winkler and H. B. Gray, *Science*, 1990, **247**, 1069-1071.

11 H. M. McConnell, *J. Chem. Phys.*, 1961, **35**, 508-515.

12 (a) P. P. Edwards, H. B. Gray, M. T. J. Lodge and R. J. P. Williams, *Angew. Chem. Int. Ed.*, 2008, **47**, 6758-6765; (b) H. B. Gray and J. R. Winkler, *Ann. Rev. Biochem.*, 1996, **65**, 537-561; (c) E. A. Weiss, M. J. Ahrens, L. E. Sinks, A. V. Gusev, M. A. Ratner and M. R. Wasielewski, *J. Am. Chem. Soc.*, 2004, **126**, 5577-5584; (d) O. S. Wenger, B. S. Leigh, R. M. Villahermosa, H. B. Gray and J. R. Winkler, *Science*, 2005, **307**, 99-102; (e) M. T. Indelli, C. Chiorboli, L. Flamigni, L. De Cola and F. Scandola, *Inorg. Chem.*, 2007, **46**, 5630-5641; (f) S. Welter, F. Lafolet, E. Cecchetto, F. Vergeer and L. De Cola, *ChemPhysChem*, 2005, **6**, 2417-2427.

13 (a) M. P. Eng and B. Albinsson, *Angew. Chem. Int. Ed.*, 2006, **45**, 5626-5629; (b) O. S. Wenger, *Acc. Chem. Res.*, 2011, **44**, 25-35; (c) K. Pettersson, J. Wiberg, T. Ljungdahl, J. Mårtensson and B. Albinsson, *J. Phys. Chem. A*, 2006, **110**, 319-326; (d) J. Chen and O. S. Wenger, *Chem. Sci.*, 2015, **6**, 3582-3592; (e) S. F. Nelsen, R. F. Ismagilov and D. R. Powell, *J. Am. Chem. Soc.*, 1998, **120**, 1924-1925.

14 C. Atienza-Castellanos, M. Wielopolski, D. M. Guldi, C. van der Pol, M. R. Bryce, S. Filippone and N. Martín, *Chem. Commun.*, 2007, 5164-5166.

15 (a) S. S. Isied, A. Vassilian, J. F. Wishart, C. Creutz, H. A. Schwarz and N. Sutin, *J. Am. Chem. Soc.*, 1988, **110**, 635-637; (b) E. H. Yonemoto, R. L. Riley, Y. I. Kim, S. J. Atherton, R. H. Schmehl and T. E. Mallouk, *J. Am. Chem. Soc.*, 1992, **114**, 8081-8087; (c) E. H. Yonemoto, G. B. Saupe, R. H. Schmehl, S. M. Hubig, R. L. Riley, B. L. Iverson and T. E. Mallouk, *J. Am. Chem. Soc.*, 1994, **116**, 4786-4795.

16 J. G. Kirkwood and F. H. Westheimer, *J. Chem. Phys.*, 1938, **6**, 506-512.

17 M. Kuss-Petermann and O. S. Wenger, *Chimia*, 2016, **70**, 177-181.

18 (a) J. Jortner, *J. Chem. Phys.*, 1976, **64**, 4860-4867; (b) P. F. Barbara, T. J. Meyer and M. A. Ratner, *J. Phys. Chem.*, 1996, **100**, 13148-13168.

19 (a) M. R. Wasielewski, *Chem. Rev.*, 1992, **92**, 435-461; (b) V. Balzani, *Electron transfer in chemistry*, VCH Wiley, Weinheim, 2001.

20 M. Tachiya and S. Murata, *J. Phys. Chem.*, 1992, **96**, 8441-8444.

21 (a) J. Hankache and O. S. Wenger, *Chem. Commun.*, 2011, **47**, 10145-10147; (b) J. Hankache, M. Niemi, H. Lemmetyinen and O. S. Wenger, *Inorg. Chem.*, 2012, **51**, 6333-6344; (c) J. Hankache, M. Niemi, H. Lemmetyinen and O. S. Wenger, *J. Phys. Chem. A*, 2012, **116**, 8159-8168; (d) J. Hankache and O. S. Wenger, *Phys. Chem. Chem. Phys.*, 2012, **14**, 2685-2692; (e) J. Hankache and O. S. Wenger, *Chem. Eur. J.*, 2012, **18**, 6443-6447.

22 M. Sjödin, S. Styring, B. Åkermark, L. C. Sun and L. Hammarström, *J. Am. Chem. Soc.*, 2000, **122**, 3932-3936.

23 (a) D. Hanss and O. S. Wenger, *Eur. J. Inorg. Chem.*, 2009, 3778-3790; (b) D. Hanss and O. S. Wenger, *Inorg. Chem.*, 2008, **47**, 9081-9084; (c) D. Hanss and O. S. Wenger, *Inorg. Chem.*, 2009, **48**, 671-680; (d) D. Hanss, M. E. Walther and O. S. Wenger, *Coord. Chem. Rev.*, 2010, **254**, 2584-2592; (e) J. Chen, M. Kuss-Petermann and O. S. Wenger, *Chem. Eur. J.*, 2014, **20**, 4098-4104; (f) J. Chen, M. Kuss-Petermann and O.

S. Wenger, *J. Phys. Chem. B*, 2015, **119**, 2263-2273; (g) M. Kuss-Petermann, H. Wolf, D. Stalke and O. S. Wenger, *J. Am. Chem. Soc.*, 2012, **134**, 12844-12854; (h) M. E. Walther and O. S. Wenger, *ChemPhysChem*, 2009, **10**, 1203-1206; (i) M. E. Walther, J. Grilj, D. Hanss, E. Vauthey and O. S. Wenger, *Eur. J. Inorg. Chem.*, 2010, 4843-4850; (j) D. Hanss, M. E. Walther and O. S. Wenger, *Chem. Commun.*, 2010, **46**, 7034-7036.

24 S. S. Isied, M. Y. Ogawa and J. F. Wishart, *Chem. Rev.*, 1992, **92**, 381-394.

25 S. S. Isied, A. Vassilian, R. H. Magnuson and H. A. Schwarz, *J. Am. Chem. Soc.*, 1985, **107**, 7432-7438.

26 A. Vassilian, J. F. Wishart, B. Vanhemelryck, H. Schwarz and S. S. Isied, *J. Am. Chem. Soc.*, 1990, **112**, 7278-7286.

27 M. Y. Ogawa, J. F. Wishart, Z. Y. Young, J. R. Miller and S. S. Isied, *J. Phys. Chem.*, 1993, **97**, 11456-11463.